NASA Technical Paper 2989

May 1990

Discrete-Vortex Model for the Symmetric-Vortex Flow on Cones

Thomas G. Gainer

NASA

NASA Technical Paper 2989

1990

Discrete-Vortex Model for the Symmetric-Vortex Flow on Cones

Thomas G. Gainer
Langley Research Center
Hampton, Virginia

National Aeronautics and Space Administration
Office of Management
Scientific and Technical Information Division

Summary

A relatively simple but accurate potential-flow model has been developed for studying the symmetric-vortex flow on cones. The model is a modified version of the model first developed by Bryson, in which discrete vortices and straight-line feeding sheets were used to represent the flow field. It differs, however, in the zero-force condition used to position the vortices and determine their circulation strengths. The Bryson model imposed the condition that the net force on the feeding sheets and discrete vortices must be zero. The proposed model satisfies this zero-force condition by having the vortices move as free vortices, at a velocity equal to the local cross-flow velocity at their centers. When the free-vortex assumption is made, a solution is obtained in the form of two nonlinear algebraic equations that relate the vortex-center coordinates and vortex strengths to the cone angle and angle of attack. The vortex-center locations calculated using the model are in good agreement with experimental values. The cone normal forces and center locations are in good agreement with the vortex cloud method of calculating symmetric flow fields.

Introduction

The symmetric-vortex flow on cones has been studied in several investigations in connection with the high-angle-of-attack performance of aircraft and missiles. Designers would like to use the lift produced by these flows to improve maneuvering capability, but they also want to understand and be able to predict adverse flow patterns, such as vortex asymmetry, that can occur. Vortex asymmetries usually occur at moderate to high angles of attack and can cause serious stability and control problems. A thorough knowledge of the symmetric-vortex flow field could lead to a better understanding of why and under what conditions these asymmetries occur.

The previous analytical studies of conical vortex flow have included Navier-Stokes solutions, obtained mainly at supersonic speeds (refs. 1 to 3), and potential-flow solutions, obtained using free-sheet methods (refs. 4 to 7). More recently, a vortex cloud method (refs. 8 and 9) has been developed that allows vortex flow characteristics to be determined for cones as well as general forebody shapes. These methods, however, involve fairly complicated time-stepping or iteration procedures, and the results available in the literature cover only a limited number of cone angles and angles of attack. The effects of the different parameters governing conical vortex flow have not been clearly defined.

This report describes a relatively simple discrete-vortex model for studying the vortex flow on cones. The model is based on the Bryson model described in references 10 and 11, but uses a different zero-force condition than that used by Bryson to locate the vortices and determine their circulation strengths. Bryson imposed the condition that there be zero net force on a system consisting of primary vortices and straight-line feeding sheets. In the present model, this zero-force condition is satisfied by having the vortices move as free vortices, that is, at velocities equal to the local flow velocities at their centers.

The assumptions of a free vortex and conical flow enable a solution to be obtained in the form of two nonlinear algebraic equations that relate vortex position, vortex strength, and the parameter $\tan\alpha/\tan\delta$. Together with information about the separation point, these relationships can be used to obtain a solution for a given cone angle and angle of attack.

The vortex centers calculated using the present method are shown to be in good agreement with the experimental data obtained at incompressible laminar-flow conditions in reference 12. When the measured separation points are used, the method gives an accurate prediction of the travel of the vortex centers as the cone goes through an angle-of-attack range. The vortex-center locations and normal forces predicted using the method also agree with those predicted using the vortex cloud method of references 8 and 9 for the same circulation strength.

Symbols

a	X-axis influence coefficient (symmetric-vortex alignment)
a_{11}, b_{11}	X- and Y-axis influence coefficients, respectively, that express influence of image of vortex 1 on conditions at center of vortex 1 for asymmetric-vortex alignment (see fig. B1)
a_{12}, b_{12}	X- and Y-axis influence coefficients, respectively, that express influence of vortex 2 and its image on conditions at vortex 1 for asymmetric-vortex alignment (see fig. B1)
a_{21}, b_{21}	X- and Y-axis influence coefficients, respectively, that express influence of vortex 1 and its image on conditions at vortex 2 for asymmetric-vortex alignment (see fig. B1)

a_{22}, b_{22} X- and Y-axis influence coefficients, respectively, that express influence of image of vortex 2 on conditions at center of vortex 2 for asymmetric-vortex alignment (see fig. B1)

b Y-axis influence coefficient (symmetric-vortex alignment)

C_k nondimensional vortex strength, $\frac{\Gamma}{2\pi r_o U_\infty \sin\alpha}$

$C_{k,\text{avail}}$ nondimensional vortex strength made available for vortex formation by boundary-layer separation on cone

$C_{k,\text{req}}$ nondimensional vortex strength required to meet the zero-force condition

C_N normal-force coefficient, $\frac{\text{Normal force}}{(1/2)\rho U_\infty^2 S}$

c_N local normal-force coefficient, measured in X-Y plane at a given z-station along cone axis, $\frac{\text{Local normal force}}{(1/2)\rho U_\infty^2 D}$

D diameter of cone base

dp differential pressure across a feeding sheet

F force exerted on vortex system by body at a given cross section

$F_{F.S.}$ pressure force on feeding sheet

F_n local normal force

F_v Kutta-Joukowski force acting at vortex center

i unit vector along imaginary axis

k vorticity reduction factor

L length of cone

MV momentum of vortex pair

r radial distance in crossflow plane, $\sqrt{x^2+y^2}$

r_o radius of cone cross section

S base area of cone

t time

U X-axis component of velocity, nondimensionalized with respect to $U_\infty \sin\alpha$, that results from free-stream flow around cone at a given cross section

U_e velocity at edge of boundary layer at a separation point on cone

U_∞ free-stream velocity

u $= \frac{\partial\phi}{\partial x}$, X-axis component of velocity at a point in flow field, nondimensionalized with respect to $U_\infty \sin\alpha$

V Y-axis component of velocity, nondimensionalized with respect to $U_\infty \sin\alpha$, that results from free-stream flow around cone at a given cross section

V_k^* induced velocity at vortex center, $u_k + iv_k$

v $= \frac{\partial\phi}{\partial y}$, Y-axis component of velocity at a point in flow field, nondimensionalized with respect to $U_\infty \sin\alpha$

w complex potential, $\phi + i\psi$

x X-axis coordinate (see fig. 1)

x' $= x/r_o$

y Y-axis coordinate (see fig. 1)

y' $= y/r_o$

z Z-axis coordinate (see fig. 1)

α cone angle of attack

Γ circulation, positive clockwise in first $(+x, +y)$ quadrant of X-Y plane

Γ_{avail} circulation made available for vortex formation by boundary-layer separation taking place on cone

δ cone semi-apex angle

ζ $= x + iy$, complex coordinate of a point in flow field

ζ_o complex coordinate of origin of feeding sheet (see fig. A1)

θ $= \tan^{-1}(\frac{y}{x})$, angle measured from positive X-axis to a point in flow field

ρ fluid density

ϕ velocity potential

ϕ_s angular distance to separation point on cone at a given cross section, measured from negative X-axis (see fig. 1)

ψ stream function

Subscripts and superscripts:

k primary vortex index

$(^-)$ complex conjugate

1 refers to conditions at center of vortex 1 (see fig. B1)

2 refers to conditions at center of vortex 2 (see fig. B1)

Mathematical Development

Basic Flow Model

The model used (see fig. 1) is the two-dimensional, discrete-vortex model that is described in reference 13 and used by a number of investigators, but with a source term added to simulate conical flow. The model assumes incompressible potential flow. The flow at each cross section is represented by two primary vortices placed at the positions x_k and $\pm y_k$ with image vortices placed inside the cone at the positions shown in figure 1 to satisfy the tangent-flow boundary condition on the surface. The added source term has a strength that varies with the distance z along the cone axis and simulates the velocities that occur normal to the surface at each cross section in conical flow. The complex potential for this system is

$$w = \phi + i\psi = U_\infty \left(\zeta + \frac{r_o^2}{\zeta}\right) + \frac{i\Gamma}{2\pi}\left[\ln\left(\zeta - \zeta_k\right) - \ln\left(\zeta - \frac{r_o^2}{\bar{\zeta}_k}\right) - \ln\left(\zeta - \bar{\zeta}_k\right) + \ln\left(\zeta - \frac{r_o^2}{\zeta_k}\right)\right] - r_o U_\infty \cos\alpha \tan\delta \ln\zeta \qquad (1)$$

The first term on the right-hand side in equation (1) is the complex potential for the free-stream flow around the cross section; the second through fifth terms are those for the primary vortices and their images; the last term is the source term added for conical flow. This source term assumes the flow is purely conical, that is, all flow quantities are constant along rays emanating from the cone apex. This term does not account for the end effects that result from the cone having a finite length. (For examples of more complex representations that do account for end effects, see ref. 14.)

The real part of equation (1) gives the velocity potential

$$\phi = U_\infty \sin\alpha \left(1 + \frac{r_o^2}{x^2 + y^2}\right) x - \frac{\Gamma}{2\pi r_o U_\infty \sin\alpha}\left[\tan^{-1}\left(\frac{y - y_k}{x - x_k}\right) - \tan^{-1}\left(\frac{y - \frac{r_o^2}{r_k^2} y_k}{x - \frac{r_o^2}{r_k^2} x_k}\right) - \tan^{-1}\left(\frac{y + y_k}{x - x_k}\right) + \tan^{-1}\left(\frac{y + \frac{r_o^2}{r_k^2} y_k}{x - \frac{r_o^2}{r_k^2} x_k}\right)\right] - r_o U_\infty \cos\alpha \tan\delta \ln\sqrt{x^2 + y^2} \qquad (2)$$

The imaginary part of equation (1) gives the stream function

$$\psi = U_\infty \sin\alpha \left(1 - \frac{r_o^2}{x^2 + y^2}\right) y + \frac{\Gamma}{2\pi}\left[\ln\sqrt{(x - x_k)^2 + (y - y_k)^2} - \ln\sqrt{\left(x - \frac{r_o^2}{r_k^2} x_k\right)^2 + \left(y - \frac{r_o^2}{r_k^2} y_k\right)^2} - \ln\sqrt{(x - x_k)^2 + (y + y_k)^2} + \ln\sqrt{\left(x - \frac{r_o^2}{r_k^2} x_k\right)^2 + \left(y + \frac{r_o^2}{r_k^2} y_k\right)^2}\right] - r_o U_\infty \cos\alpha \tan\delta \tan\theta \qquad (3)$$

The nondimensional velocity in the x direction, written in terms of x' and y' coordinates is given by

$$u = r\left[1 - \frac{1}{x'^2 + y'^2} + \frac{2y'^2}{\left(x'^2 + y'^2\right)^2}\right]$$

$$+ \frac{\Gamma}{2\pi r_o U_\infty \sin\alpha}\left[\frac{(y' - y'_k)}{(x' - x'_k)^2 + (y' - y'_k)^2}\right.$$

$$- \frac{\left(y' - \frac{r_o^2}{r_k^2}y'_k\right)}{\left(x' - \frac{r_o^2}{r^2}x'_k\right)^2 + \left(y' - \frac{r_o^2}{r^2}y'_k\right)^2}$$

$$- \frac{(y' + y'_k)}{(x'_k - x')^2 + (y'_k + y')^2}$$

$$\left. + \frac{\left(y' + \frac{r_o^2}{r_k^2}y'_k\right)}{(x' - x'_k)^2 + \left(y' + \frac{r_o}{r_k^2}y'_k\right)^2}\right]$$

$$+ \frac{\tan\delta}{\tan\alpha}\frac{\cos\theta}{\sqrt{x'^2 + y'^2}} \qquad (4)$$

This velocity can be written as

$$u = U + aC_k + \frac{\tan\delta}{\tan\alpha}\frac{\cos\theta}{\sqrt{x'^2 + y'^2}} \qquad (5)$$

where a is an X-axis influence coefficient equal to the sum of the terms multiplied by $\frac{\Gamma}{2\pi r_o U_\infty \sin\alpha}$ in equation (4).

The velocity in the y-direction is given by

$$v = -2\frac{x'y'}{\left(x'^2 + y'^2\right)^2} + \frac{\Gamma}{2\pi r_o U_\infty \sin\alpha}\left[\frac{-(x' - x'_k)}{(x' - x'_k)^2 + (y' - y'_k)^2}\right.$$

$$+ \frac{\left(x' - \frac{r_o^2}{r_k^2}x'_k\right)}{\left(x' - \frac{r_o^2}{r_k^2}x'_k\right)^2 + \left(y' - \frac{r_o^2}{r_k^2}y'_k\right)^2}$$

$$\left. + \frac{(x' - x'_k)}{(x' - x'_k)^2 + (y' + y'_k)^2} - \frac{\left(x' - \frac{r_o^2}{r_k^2}x'_k\right)}{\left(x' - \frac{r_o^2}{r_k^2}x'_k\right)^2 + \left(y' + \frac{r_o^2}{r_k^2}y'_k\right)^2}\right]$$

$$+ \frac{\tan\delta}{\tan\alpha}\frac{\sin\theta}{\sqrt{x'^2 + y'^2}} \qquad (6)$$

This velocity can be written as

$$v = V + bC_k + \frac{\tan\delta}{\tan\alpha}\frac{\sin\theta}{\sqrt{x'^2 + y'^2}} \qquad (7)$$

where b is a Y-axis-oriented influence coefficient equal to the sum of the terms multiplied by $\frac{\Gamma}{2\pi r_o U_\infty \sin\alpha}$ in equation (6).

Solution for Conical Flow

The basic flow problem can be solved if the locations and circulation strengths of the primary vortices are known. Equation (2) defines a velocity potential ϕ that is a function of x and y and satisfies the Laplace equation and the boundary conditions of the problem. The Laplace equation is automatically satisfied because each of the singularities involved satisfies the Laplace equation. One boundary condition—that the flow must be tangent to the body at the surface—is satisfied by the image system used. The other boundary condition—that the flow velocity at infinity must be equal to the free-stream velocity—is satisfied because the velocity induced by each of the singularities varies inversely with the distance from the singularity.

Once this velocity potential is defined, the velocities at different points in the potential flow field and the forces on the body can be determined. The problem then becomes one of determining the locations and circulation strengths of the vortex centers for different cone angles and angles of attack. These locations and strengths are usually determined by imposing a zero-force condition to constrain the motion of the primary vortices.

Zero-Force Condition

The zero-force condition imposed in the present method is that the primary vortices move as free vortices, that is, at a velocity equal to the local fluid velocity of the vortex centers. This condition is expressed mathematically by

$$V_k^* = \frac{d\zeta_k}{dt} \qquad (8)$$

This condition is a departure from the zero-force condition used by Bryson and others (e.g., see refs. 7 and 10), for which the force on a feeding sheet that extends into the vortex is balanced out by an equal and opposite force at the vortex center; thus, there is no net force on the vortex system. However, the use of equation (8) is justified in appendix A.

Conical Flow Assumptions

Equation (8) relates the induced velocity at the vortex center to the absolute velocity $\frac{d\zeta_k}{dt}$ of the center relative to the axis-system origin. This absolute velocity can be expressed in terms of cone semi-apex angle and angle of attack by assuming conical flow and making use of the impulsive-flow analogy. According to the impulsive-flow analogy (e.g., ref. 15), the flow at a given cross section of the cone is equivalent to that about a two-dimensional cylinder whose radius is expanding with time, where time in the two-dimensional plane is related to the distance along the axis of the three-dimensional cone by

$$t = \frac{z}{U_\infty \cos\alpha} \tag{9}$$

If the flow is assumed to be conical, the movement of the vortex center is known. The center moves radially away from the cone axis as either time (in the two-dimensional plane) or distance z (along the three-dimensional body) increases. Therefore, the velocity of the vortex center at a given cross section must point in the radial direction and have a magnitude of

$$\frac{dr_k}{dt} = U_\infty \cos\alpha \left(\frac{dr_k}{dz}\right) \tag{10}$$

Now the derivative with respect to z can be written as

$$\frac{dr_k}{dz} = \left(\frac{dr_k}{dr_o}\right)\left(\frac{dr_o}{dz}\right) = \left(\frac{dr_k}{dr_o}\right)\tan\delta \tag{11}$$

Since, for conical flow, the nondimensional distance to the vortex center remains constant for a given cone angle and angle of attack,

$$\frac{dr_k}{dt} = \left(\frac{r_k}{r_o}\right)\tan\delta\, U_\infty \cos\alpha \tag{12}$$

The velocity of the vortex center, nondimensionalized with respect to $U_\infty \sin\alpha$, can therefore be written as

$$\frac{1}{U_\infty \sin\alpha}\left(\frac{dr_k}{dt}\right) = \left(\frac{r_k}{r_o}\right)\frac{\tan\delta}{\tan\alpha} \tag{13}$$

Equations for C_k and $\tan\alpha/\tan\delta$

In terms of nondimensionalized X- and Y-axis velocity components, the zero-force condition (eq. (8)) becomes

$$U_k + a_k C_k + \frac{\tan\delta}{\tan\alpha}\left(\frac{\cos\theta_k}{r_k/r_o}\right) = \left(\frac{r_k}{r_o}\right)\frac{\tan\delta}{\tan\alpha}\cos\theta_k \tag{14}$$

$$V_k + b_k C_k + \frac{\tan\delta}{\tan\alpha}\left(\frac{\sin\theta_k}{r_k/r_o}\right) = \left(\frac{r_k}{r_o}\right)\frac{\tan\delta}{\tan\alpha}\sin\theta_k \tag{15}$$

(For an extension of the zero-force equations (eqs. (14) and (15)) to asymmetric-vortex alignments, see appendix B.) Here, $C_{k,\mathrm{req}}$ is a required nondimensional vortex strength—it is needed to meet the zero-force condition for a given vortex-center location. The influence coefficients a_k and b_k in equations (14) and (15) omit the respective terms $\frac{y'-y'_k}{(x'-x'_k)^2+(y'-y'_k)^2}$ (see eq. (4)) and $\frac{-(x'-x'_k)}{(x'-x'_k)^2+(y'-y'_k)^2}$ (see eq. (6)) since, in potential flow calculations, it can be assumed that a discrete straight-line vortex has no influence on itself. (See ref. 16.)

Combining the terms containing $\tan\alpha/\tan\delta$ and dividing equation (15) by equation (14) gives

$$\frac{V_k + b_k C_k}{U_k + a_k C_k} = \tan\theta_k \tag{16}$$

from which the circulation required to meet the zero-force condition can be determined as

$$C_{k,\mathrm{req}} = \frac{-(U_k \tan\theta_k - V_k)}{(a_k \tan\theta_k - b_k)} \tag{17}$$

Since the factors defining the nondimensional vortex strength in equation (17)—U_k, V_k, a_k, and b_k—are functions of x_k and y_k only, this nondimensional strength is uniquely defined by the vortex-center location.

The value of $\tan\alpha/\tan\delta$ corresponding to a given vortex-center location and nondimensional vortex strength can be determined from either equation (14) or (15) as follows:

$$\frac{\tan\alpha}{\tan\delta} = \frac{(r_k/r_o) - \left(\frac{1}{r_k/r_o}\right)\cos\theta_k}{(U_k + a_k C_k)} = \frac{(r_k/r_o) - \left(\frac{1}{r_k/r_o}\right)\sin\theta_k}{(V_k + b_k C_k)} \tag{18}$$

Equations (17) and (18) form the basis of the present method; they provide two equations in terms of the known parameter $\tan\alpha/\tan\delta$ and the three unknown parameters x'_k, y'_k, and $C_{k,\mathrm{req}}$. A third equation that is available for solving the problem is an equation for the vortex strength. The nondimensional vortex strength given by equation (17) is that required to meet the zero-force condition, but just what value this strength achieves for a given value of $\tan\alpha/\tan\delta$ depends on how much circulation is made available for vortex formation by the boundary-layer separation that is taking place on the cone. This available circulation can be determined from the rate

at which circulation is generated at the separation points on the cone.

Determination of Available Circulation

If the location of the separation point on the cone is known, having been either measured or calculated using a boundary-layer-separation criterion such as that employed in the vortex cloud program of references 8 and 9, then the rate at which circulation is generated can be approximated by the relationship:

$$\frac{d\Gamma_{\text{avail}}}{dt} = k\left(\frac{U_e^2}{2}\right) \tag{19}$$

where U_e is the edge velocity at the separation point (it includes the velocities induced by the vortices). The k factor is a vorticity modification factor that accounts for the fact that, in general, not all the vorticity generated by the boundary-layer separation is entrained into the primary vortices. A k factor of 0.6 is usually assumed. (See ref. 8.)

Since, for conical flow, Γ varies linearly with t,

$$\frac{d\Gamma_{\text{avail}}}{dt} = \frac{\Gamma_{\text{avail}}}{t} \tag{20}$$

By using equation (9), equation (19) can be written as

$$C_{k,\text{avail}} = \frac{k}{4\pi}\left(\frac{U_e}{U_\infty \sin\alpha}\right)^2 \frac{\tan\alpha}{\tan\delta} \tag{21}$$

which is the nondimensional vortex strength available for a given value of $\tan\alpha/\tan\delta$.

Calculation of Normal-Force Coefficients

Once the nondimensional vortex strengths and locations of the vortex centers have been determined, the normal forces on the cone can be calculated from the equations derived in appendix C. The equation used for calculating the local normal-force coefficient at a given cross section is

$$c_N = 2\pi\left[1 + 4\left(\frac{r_k}{r_o} - \frac{1}{r_k/r_o}\right)C_k \sin\theta_k\right]\frac{z}{L}\tan\delta\sin\alpha\cos\alpha \tag{22}$$

The equation for the normal-force coefficient for the complete cone is

$$C_N = 2\left[1 + 4\left(\frac{r_k}{r_o} - \frac{1}{r_k/r_o}\right)C_k \sin\theta_k\right]\sin\alpha\cos\alpha \tag{23}$$

Results and Discussion

Vortex-Center Locations as a Function of C_k and $\tan\alpha/\tan\delta$

In the present method, the primary vortices are kept force-free by having them move as free vortices, that is, at a velocity equal to the local crossflow velocity at their centers. The vortex-center positions and circulation strengths needed to meet this condition for different cone angles and angles of attack are shown in figure 2. Figure 2 shows contours, obtained by iteration from equations (17) and (18), of constant circulation strength (solid lines) and the values of $\tan\alpha/\tan\delta$ (dashed lines); these contours are plotted as functions of the coordinates of the primary vortex center, x_k' and y_k'. Figure 2 can be used in two ways. If the available circulation strength has been determined for a given cone angle and angle of attack—either by a boundary-layer calculation or by experiment—the contours in figure 2 can be used to locate the coordinates of the vortex center. If, on the other hand, the vortex-center location has been measured experimentally, these contours can be used to approximate the circulation strengths of the vortices. In either case, the complete potential-flow field can be mapped out, and forces on the body can be determined.

The curves in figure 2 show a limit to vortex-center travel. The vortex centers would not be expected to go beyond the curve for which $\tan\alpha/\tan\delta$ is infinite (a cone angle of attack of 90°). The curve that defines this limit is the so-called Föppl curve. (See refs. 13 and 17.) The Föppl curve gives the locations of the vortex centers for which the velocity V_k^* at the center is zero for a constant-diameter cylinder in two-dimensional flow. It can be shown that this condition corresponds to having the denominators in the equations for $\tan\alpha/\tan\delta$ (eqs. (18)) equal to zero, which would produce an infinite value of $\tan\alpha/\tan\delta$. The Föppl curve, therefore, defines the limit of vortex-center travel for conical flow.

Comparison of Calculated Center Locations With Experiment

Figure 3 shows measured vortex-center locations from reference 12 superimposed on the constant C_k and $\tan\alpha/\tan\delta$ curves of figure 2. The experimental results were obtained in a water tunnel at a Reynolds number (based on cone length) of about 2.7×10^4. (The boundary layers for this condition were described in ref. 12 as being steady and laminar.) The results are shown for cone semi-apex angles of 7.5° and 12.5° in figures 3(a) and 3(b), respectively. The values of $\tan\alpha/\tan\delta$ for individual data points are indicated in the figures. These results show that as the angle of attack is increased, the vortex center moves upward, toward curves for higher values of C_k, and to the right, toward curves for higher values of $\tan\alpha/\tan\delta$. For both cones, the measured vortex-center location for a given value of $\tan\alpha/\tan\delta$

is approximately that needed to meet the zero-force requirement of the present method. At a value of $\tan\alpha/\tan\delta$ of approximately 2.0, for example, the experimental data indicate a vortex-center location at about $x_k/r_o = 1.16$ and $y_k/r_o = 0.33$; these values are in good agreement with those needed to meet the zero-force requirement.

The nondimensional vortex strengths of the primary vortices for the test results shown in figure 3 were not defined in reference 12; however, they were calculated in the present investigation by using the measured separation point locations given in reference 12. These measured locations are shown for the 7.5° and 12.5° cones in figure 4(a). The vortex strengths for a given value of $\tan\alpha/\tan\delta$ and a given separation point were determined by constructing, for that value of $\tan\alpha/\tan\delta$, a curve of y_k/r_o versus x_k/r_o similar to those shown in figures 2 and 3, and then iterating along this curve until the vortex strength required to meet the zero-force condition (eq. (17)) matched that being made available at the separation point (eq. (21)). The nondimensional vortex strengths determined by this iteration procedure for the two cones are presented in figure 4(b), which shows that this vortex strength was approximately a linear function of $\tan\alpha/\tan\delta$.

Figures 5(a) and 5(b) compare the nondimensional vortex strengths given in figure 4(b) with those determined by using the Bryson equations; these figures also compare the vortex-center locations determined by each method with the experimental-center locations obtained from reference 12. The vortex-center locations calculated using the present method are in generally good agreement with the measured values over the range of values of $\tan\alpha/\tan\delta$ shown. The predictions made with the Bryson method, on the other hand, were not nearly as good. Because of the relationship between ϕ_s and $\tan\alpha/\tan\delta$ contained in the Bryson zero-force equation, solutions with the Bryson method were possible for only certain segments of the curves of ϕ_s versus $\tan\alpha/\tan\delta$ shown in figure 4(a). That is, for the 7.5° cone, solutions were possible only for values of $\tan\alpha/\tan\delta$ between about 3.6 and 4.4; for the 12.5° cone, no solutions were possible over the complete range of values of $\tan\alpha/\tan\delta$ for which data were taken. The nondimensional vortex strengths determined by the Bryson method were significantly higher than those determined by the present method. The vortex-center locations were much farther away from the axis of asymmetry for a given value of $\tan\alpha/\tan\delta$ than indicated by either the present calculations or the experimental data.

Comparison With Vortex Cloud Results

To further verify the basic assumption of the present method—for the cone, the vortices remain force-free by traveling with the local crossflow velocity—calculations made using the present method are compared in this section with predictions made using the vortex cloud method of references 8 and 9. The vortex cloud method uses discrete vortices generated at the separation points on the body to model the vortex wake. These discrete vortices are assumed to travel at the local crossflow velocity and eventually wrap up into the equivalent of the primary vortices modeled in the present investigation. The method uses a modified Stratford separation criterion to determine the locations of the separation points and assumes circulation is generated at the rate indicated by equation (19) at these points. To provide a common basis of comparison for the two methods, the calculations for both are based on the separation-point locations and nondimensional vortex strengths determined by the vortex cloud method.

The flow fields depicted by the two methods are compared in figure 6. The points indicated by the symbols are the locations of the individual vortex elements used in the vortex cloud method. The streamlines indicated in figure 6 are those calculated using the present method. (The streamlines shown are not actually streamlines, but rather, projections in the crossflow plane of the paths followed by individual particles in the three-dimensional flow.) The vortex-center locations indicated by the two methods are in good agreement for the three angles of attack shown.

Normal-force coefficients calculated using the present method and the vortex cloud method are compared in figures 7 to 9. Figure 7 shows the variations of local normal-force coefficient c_N with distance along the body z/L for different angles of attack. Figures 8 and 9 show the variations in total normal-force coefficient with $\tan\alpha/\tan\delta$ for cone semi-apex angles of 5° and 7.5°, respectively. The nondimensional vortex strengths used in obtaining these results were those determined for the different cone angles and angles of attack by the vortex cloud program; these strengths are shown as a function of $\tan\alpha/\tan\delta$ in figures 8(a) and 9(a).

Figure 7 shows generally good agreement between the local normal-force coefficients calculated using the two methods, based on the same nondimensional vortex strength. The local normal-force coefficients calculated using the vortex cloud method show some oscillation with increasing values of z/L, particularly for the 5° cone. This oscillation is probably the result of errors in the iteration procedure used in the vortex cloud calculations for these particular cases. The

present method shows a straight-line variation in c_N with z/L, which is in keeping with the conical-flow assumptions on which the method is based.

To indicate the level of the normal force produced by vortex flow on the two cones, figures 8 and 9 show the attached-flow normal-force coefficients (the normal-force coefficients for the cones without vortex flow, as determined from slender-body theory) and the total normal-force coefficients (the sum of the attached-flow and vortex-flow normal-force coefficients). Figures 8 and 9 show that the nondimensional vortex strengths—as calculated by the vortex cloud method—were slightly higher for the 7.5° cone than for the 5° cone at a given value of $\tan\alpha/\tan\delta$. These higher values of C_k resulted in a noticeably higher level of total normal force for the 7.5° cone. The normal-force coefficients for the vortex cloud method were generally lower than those calculated by the present method. At least some of this lower level of overall normal force was the result of a lower level of local normal force produced toward the end of the cone by end effects. The overall level of agreement, however, was good.

Conclusions

A potential-flow model has been developed for studying the symmetric-vortex flow on cones. The model assumes conical flow conditions and satisfies the zero-force condition on the primary vortices by having them move at the local induced-flow velocity. The solution obtained is in the form of two nonlinear algebraic equations that relate the vortex-center locations, the vortex strengths, and the ratio of the tangent of the angle of attack to the tangent of the cone semi-apex angle $\tan\alpha/\tan\delta$. The following conclusions can be derived from the results of this investigation:

1. The assumption that the vortex maintains a zero-force condition by being a free vortex, that is, by moving at a velocity equal to the local crossflow velocity, appears valid.
2. When measured separation-location points were used to calculate the available circulation, the vortex-center locations calculated using the present method were in good agreement with low-speed laminar water-tunnel data.
3. The vortex-center locations and normal forces calculated using this method were in good agreement with those calculated using the vortex cloud method of references 8 and 9 for the same vortex strengths.

NASA Langley Research Center
Hampton, VA 23665-5225
March 22, 1990

Appendix A

Justification for Zero-Force Condition Used in Present Method

Zero-Force Condition Used by Bryson

The zero-force condition used to determine vortex positions and strengths in a concentrated vortex model is based on the principle that an isolated potential vortex should sustain no force. (See ref. 7.) In the Bryson method (ref. 10), the zero-force equation is developed by installing a feeding sheet (fig. A1) and balancing out the force on the feeding sheet with an equal and opposite force on the vortex. This feeding sheet is assumed to be the path along which vorticity is fed into the primary vortex and acts as a mathematical branch cut, which is needed to make the velocity potential for the system single-valued. There is a discontinuity in ϕ equal to the circulation strength across this branch cut, and since Γ varies with distance along the cone axis, ϕ also varies with this distance. Since time and distance along the cone axis are related (see eq. (9) of text), there will be, according to the unsteady Bernoulli equation, a pressure difference across the feeding sheet of

$$dp = \rho \frac{d\Gamma}{dt} \tag{A1}$$

When integrated over the length of the feeding sheet, this pressure difference results in a pressure force of

$$F_{F.S.} = -i\rho \frac{d\Gamma}{dt} (\zeta_k - \zeta_o) \tag{A2}$$

Bryson required that this force be balanced out by an equal and opposite force at the vortex center.

The force at the vortex center arises from a nonzero local-flow velocity at the center, and according to the Kutta-Joukowski theorem, is given by

$$F_v = i\rho\Gamma \left(V_k^* - \frac{d\zeta_k}{dt} \right) \tag{A3}$$

This force consists of two parts: (1) the force $i\rho\Gamma V_k^*$ is due to the induced effects at the vortex center. (Here, V_k^*, the induced velocity, is equal to the free-stream crossflow velocity plus the velocities induced by all of the singularities in the system, except the primary vortex itself; the velocity induced by a primary vortex at its own center is assumed to be zero.) (2) The force $-i\rho\Gamma \frac{d\zeta_k}{dt}$ is due to the absolute motion of the vortex center.

Combining equations (A2) and (A3) gives the following zero-force equation used by Bryson:

$$-i\rho \frac{d\Gamma}{dt} (\zeta_k - \zeta_o) + i\rho\Gamma \left(V_k^* - \frac{d\zeta_k}{dt} \right) = 0 \tag{A4}$$

Zero-Force Condition Used in Present Method

The zero-force equation used by Bryson represents one way of resolving the problem of how to make the velocity potential single-valued and at the same time ensure zero net force on the vortex system. This solution is not completely satisfactory, however, since it requires a pressure force on the feeding sheet that is balanced out only "in the mean" to get zero net force on the vortex system. In the present paper, a new approach is taken; the branch cut is assumed to lie between the primary vortex and its image (instead of between the primary vortex and a separation point). Then, when the equation for the forces on the vortex system is written out, it shows that the pressure force on the branch cut is actually part of the change in momentum that the vortex system undergoes in response to the force exerted on it by the body. Therefore, the pressure force should not be balanced out. (See fig. (A2).)

The momentum of a pair of vortices of equal circulation strength is equal to the product of the fluid density, the circulation, and the distance between the vortices. (See refs. 18 and 19.) For the system shown in figure (A2), the total momentum is given by the following:

$$MV = i\rho\Gamma \left(\zeta_k - \frac{r_o^2}{\bar{\zeta}_k} \right) - i\rho\Gamma \left(\bar{\zeta}_k - \frac{r_o^2}{\zeta_k} \right) \tag{A5}$$

The force F that the body exerts on the fluid is equal to the rate of change of momentum. Taking the derivative of MV with respect to time and expanding the results gives

$$F = i\rho \frac{d\Gamma}{dt} \left(\zeta_k - \frac{r_o^2}{\bar{\zeta}_k} \right) - i\rho \frac{d\Gamma}{dt} \left(\bar{\zeta}_k - \frac{r_o^2}{\zeta_k} \right) + i\rho\Gamma \frac{d\zeta_k}{dt}$$

$$- i\rho\Gamma \frac{d\bar{\zeta}_k}{dt} - i\rho\Gamma \frac{d}{dt} \left(\frac{r_o^2}{\bar{\zeta}_k} \right) + i\rho\Gamma \frac{d}{dt} \left(\frac{r_o^2}{\zeta_k} \right) \tag{A6}$$

If the branch cuts are taken between the primary vortices and their images, as shown in figure (A2), the first term in equation (A6) can be interpreted as a force on the upper branch cut and the second term as a force on the lower branch cut. These forces are of the same form as Bryson's feeding-sheet

force (eq. (A2)), but they act over the distance between the primary and image vortices instead of the length $\zeta_k - \zeta_o$. The terms $i\rho\Gamma\frac{d\zeta_k}{dt}$ and $-i\rho\Gamma\frac{d\bar{\zeta}_k}{dt}$ in equation (A6) can be interpreted as forces caused by the absolute motion of the primary vortices; likewise, the terms $-i\rho\Gamma\frac{d}{dt}\left(\frac{r_o^2}{\zeta_k}\right)$ and $i\rho\Gamma\frac{d}{dt}\left(\frac{r_o^2}{\bar{\zeta}_k}\right)$ can be interpreted as forces associated with the motion of the image vortices. (These forces are shown as dashed vectors in fig. (A2) because, in accordance with d'Alembert's principle, they are effective forces, equal but opposite in direction to rates of change in momentum, rather than actual forces.)

The effective forces shown in figure (A2) combine with the force F that the body exerts on the fluid to form a system in equilibrium. Since these forces are in equilibrium, there cannot be an additional force that is due to induced effects acting at the vortex center; if there were, the force on the body would not be equal to that given by the momentum theorem.

The zero-force condition to impose with the vortex system in figure (A2), therefore, is that there can be no force due to induced effects acting at the vortex center. For the cone in the present study, this condition was imposed by requiring that each primary vortex move as a free vortex, that is, at a velocity equal to the local flow velocity at its center:

$$V_k^* = \frac{d\zeta_k}{dt} \tag{A7}$$

In the present method, the feeding sheet has essentially been removed from consideration; a feeding sheet per se is not considered necessary with this type of concentrated vortex model. The branch cut from the primary vortex center to its image vortex center serves to make the velocity potential single-valued. And while the vortices are assumed to be fed in some way so that their circulation strengths increase with distance along the cone axis, the actual manner in which they are fed is not considered important. In the actual flow, vorticity is fed into primary vortices along curved feeding sheets, as best depicted in the vortex cloud or the free vortex sheet methods. In those methods, however, as in the present method, there are no pressure forces associated with the feeding sheets that would have to be balanced out by a force on the vortex. The curved sheets in those methods are assumed to be free surfaces that cannot sustain a pressure force.

Also, the requirement that there be no force due to induced effects at the vortex center does not necessarily mean that the vortex moves with the local crossflow velocity in all types of flow fields. In an unsteady flow field, the vortex velocity must be equal to the local flow velocity at a given instant; however, since the vortex can also undergo motions caused by unsteady effects, the vortex velocity, in general, is not equal to the local flow velocity. The requirement of equation (A7), therefore, does not necessarily apply to problems such as the vortex flow over cylinders and narrow delta wings, where other constraints on the vortex system may have to be considered.

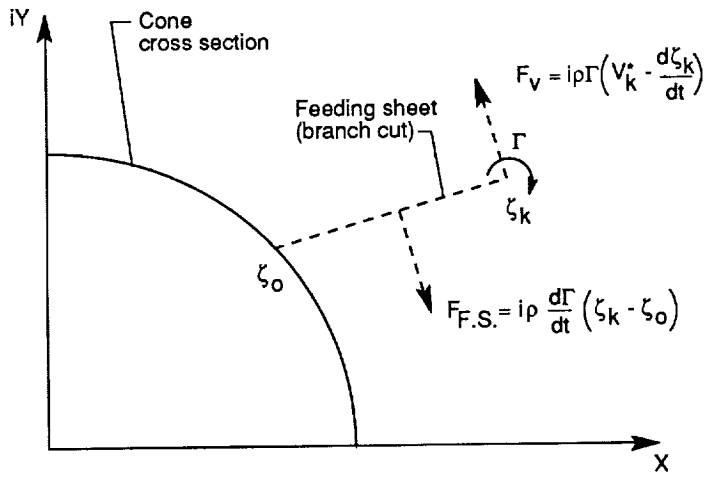

Figure A1. Forces on feeding sheet and vortex assumed in Bryson method. (Upper half of vortex system.)

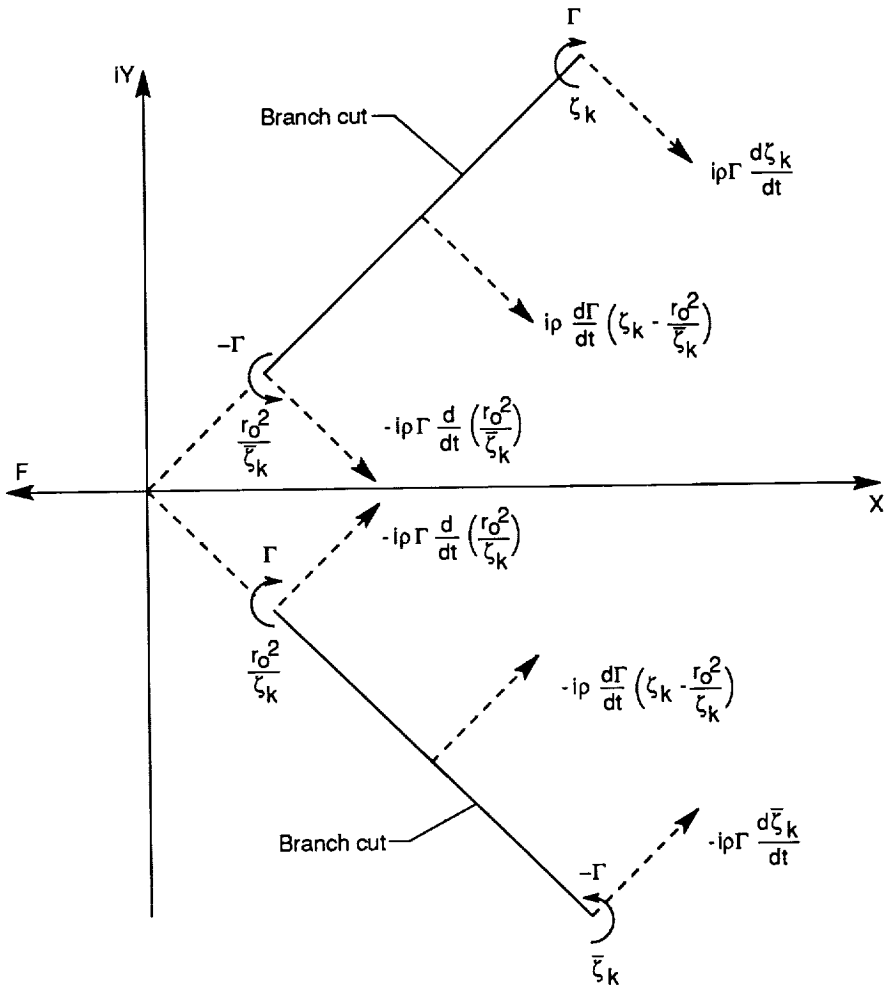

Figure A2. Branch cuts and forces assumed in present method. (Complete vortex system.)

Appendix B

Extension of Zero-Force Condition to Asymmetric Vortices

The zero-force condition on which the present method is based—that the primary vortices move as free vortices—can be extended to include vortices that have different circulation strengths and are asymmetrically aligned about the $y = 0$ axis. (See fig. B1.) This is done by writing a zero-force equation similar to equations (14) and (15) at each of the two primary vortex centers as follows:

At vortex 1,

$$U_1 + a_{11}C_{k1} + a_{12}C_{k2} = \left(\frac{r_1}{r_o} - \frac{1}{r_1/r_o}\right)\frac{\tan\delta}{\tan\alpha}\cos\theta_1 \quad \text{(B1)}$$

$$V_1 + b_{11}C_{k1} + b_{12}C_{k2} = \left(\frac{r_1}{r_o} - \frac{1}{r_1/r_o}\right)\frac{\tan\delta}{\tan\alpha}\sin\theta_1 \quad \text{(B2)}$$

At vortex 2,

$$U_2 + a_{21}C_{k1} + a_{22}C_{k2} = \left(\frac{r_2}{r_o} - \frac{2}{r_2/r_o}\right)\frac{\tan\delta}{\tan\alpha}\cos\theta_2 \quad \text{(B3)}$$

$$V_2 + b_{21}C_{k1} + b_{22}C_{k2} = \left(\frac{r_2}{r_o} - \frac{1}{r_2/r_o}\right)\frac{\tan\delta}{\tan\alpha}\sin\theta_2 \quad \text{(B4)}$$

Combining equations (B1) and (B2) gives the following equation:

$$(a_{11}\tan\theta_1 - b_{11})C_{k1} + (a_{12}\tan\theta_1 - b_{12})C_{k2} = -(U_1\tan\theta_1 - V_1) \quad \text{(B5)}$$

Combining equations (B3) and (B4) gives the following equation:

$$(a_{21}\tan\theta_2 - b_{21})C_{k1} + (a_{22}\tan\theta_2 - b_{22})C_{k2} = -(U_2\tan\theta_2 - V_2) \quad \text{(B6)}$$

Equations (B5) and (B6) can be solved simultaneously to give the circulation strengths C1 and C2 for assumed primary vortex positions. Equations (B1) and (B3) can then be solved to give the following values of $\tan\alpha/\tan\delta$ (designated by subscripts 1 and 2 for vortices 1 and 2, respectively).

From equation (B1),

$$\left(\frac{\tan\alpha}{\tan\delta}\right)_1 = \frac{\left(r_1/r_o - \frac{1}{r_1/r_o}\right)\cos\theta_1}{U_1 + a_{11}C_{k1} + a_{12}C_{k2}} \quad \text{(B7)}$$

From equation (B3),

$$\left(\frac{\tan\alpha}{\tan\delta}\right)_2 = \frac{\left(r_2/r_o - \frac{1}{r_2/r_o}\right)\cos\theta_2}{U_2 + a_{21}C_{k1} + a_{22}C_{k2}} \quad \text{(B8)}$$

A solution is obtained when the vortex centers are located such that

$$\left(\frac{\tan\alpha}{\tan\delta}\right)_1 = \left(\frac{\tan\alpha}{\tan\delta}\right)_2 \quad \text{(B9)}$$

Asymmetric solutions have been obtained using the basic Bryson equations in reference 20. Solutions using the general asymmetric form of the present method have been obtained in reference 21.

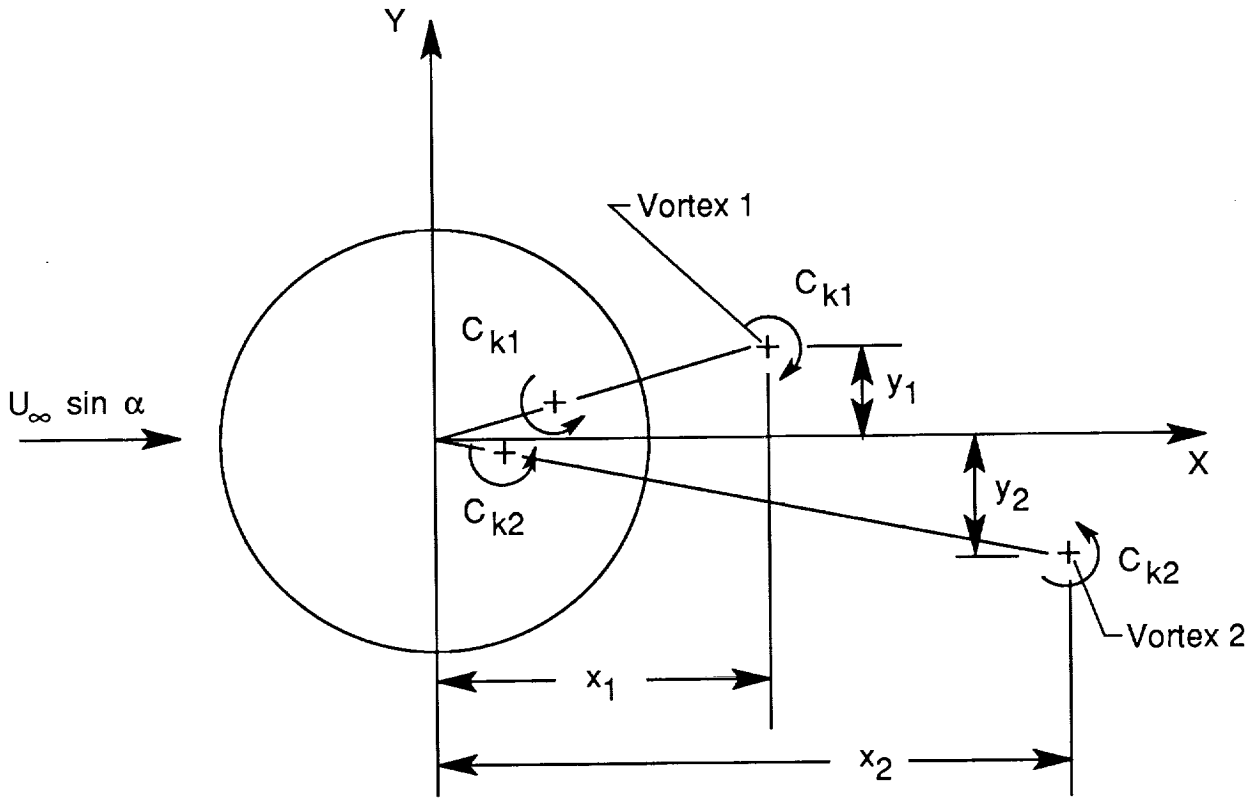

Figure B1. Asymmetric-vortex alignment at a cross section.

Appendix C

Derivation of Equations for Cone Normal Force

The normal force for the cone with vortex flow is determined from the rate of change in the momentum of the vortex system at a given cross section. The momentum of a pair of vortices is equal to the fluid density times the product of their circulation and the distance between them. (See refs. 18 and 19.) Since two pairs of vortices are involved—two primary vortices and their images—the total momentum for the vortex system at a given cross section can be written, in terms of the real variables r_k and r_o, as

$$MV = 2\rho\Gamma\left(r_k - \frac{r_o^2}{r_k}\right) \tag{C1}$$

where the momentum is directed normal to the line between the image and the primary vortex. The normal force is the rate of change of this momentum in the x-direction and is given by

$$F_n = 2\rho\left(\frac{d}{dt}\right)\left[\Gamma\left(r_k - \frac{r_o^2}{r_k}\right)\right]\sin\theta_k \tag{C2}$$

Taking the derivative with respect to t gives

$$F_n = 2\rho\left(\frac{r_k}{r_o} - \frac{1}{r_k/r_o}\right)\left(\frac{dr_o}{dt}\Gamma + \frac{r_o\, d\Gamma}{dt}\right)\sin\theta_k \tag{C3}$$

Since r_o, r_k, and Γ vary linearly with time, the following relationships can be substituted into equation (C3):

$$t = \frac{r_o}{r_o/dt} \tag{C4}$$

$$\frac{dr_o}{dt} = \frac{dr_o}{dz}\left(\frac{dz}{dt}\right) = U_\infty \tan\delta\cos\alpha \tag{C5}$$

$$\frac{d\Gamma}{dt} = \frac{\Gamma}{t} = \frac{\Gamma}{r_o}(U_\infty)\tan\delta\cos\alpha \tag{C6}$$

The local normal-force coefficient then becomes

$$c_N = \frac{F_n}{(1/2)\rho U_\infty^2 D} = \frac{16\pi r_o}{D}\left(\frac{r_k}{r_o} - \frac{1}{r_k/r_o}\right) C_k \tan\delta\sin\alpha\cos\alpha\sin\theta_k \tag{C7}$$

Since

$$\frac{r_o}{D} = \frac{z\tan\delta}{2L\tan\delta} = \frac{z}{2L} \tag{C8}$$

equation (C7) can be written as

$$c_N = 8\pi\left(\frac{r_k}{r_o} - \frac{1}{r_k/r_o}\right)\frac{z}{L}C_k\tan\delta\sin\alpha\cos\alpha\sin\theta_k \tag{C9}$$

When equation (C9) is added to the usual (slender-body) value of local normal-force coefficient, the equation for local normal-force coefficient becomes

$$c_N = 2\pi\left[1 + 4\left(\frac{r_k}{r_o} - \frac{1}{r_k/r_o}\right)C_k\sin\theta_k\right]\frac{z}{L}\tan\delta\sin\alpha\cos\alpha \tag{C10}$$

The normal-force coefficient for the complete cone is

$$C_N = \frac{D}{S}\int_0^L c_N\, dz = 2\left[1 + 4\left(\frac{r_k}{r_o} - \frac{1}{r_k/r_o}\right)C_k\sin\theta_k\right]\sin\alpha\cos\alpha \tag{C11}$$

which is equivalent to the equation used by Bryson in reference 10.

References

1. McRae, David S.: *The Conically Symmetric Navier Stokes Numerical Solution for Hypersonic Cone Flow at High Angle of Attack.* AFFDL-TR-76-139, U.S. Air Force, Mar. 1977. (Available from DTIC as AD A042 072.)
2. McRae, D. S.; Peake, D. J.; and Fisher, D. F.: A Computational and Experimental Study of High Reynolds Number Viscous/Inviscid Interaction About a Cone at High Angle of Attack. AIAA-80-1422, July 1980.
3. Peake, David J.; Owen, F. Kevin; and Higuchi, Hiroshi: Symmetrical and Asymmetrical Separations About a Yawed Cone. *High Angle of Attack Aerodynamics,* AGARD-CP-247, Jan. 1979, pp. 16-1–16-27.
4. Fiddes, S. P.: A Theory of the Separated Flow Past a Slender Elliptic Cone at Incidence. *Computation of Viscous-Inviscid Interactions,* AGARD-CP-291, Feb. 1981, pp. 30-1–30-14.
5. Smith, J. H. B.: Theoretical Modelling of Three-Dimensional Vortex Flows in Aerodynamics. *Aerodynamics of Vortical Type Flows in Three Dimensions,* AGARD-CP-342, July 1983, pp. 17-1–17-21.
6. Dyer, D. E.; Fiddes, S. P.; and Smith, J. H. B.: *Asymmetric Vortex Formation From Cones at Incidence—A Simple Inviscid Model.* Tech. Rep. 81130, British Royal Aircraft Establ., Oct. 1981.
7. Smith, J. H. B.: *Improved Calculations of Leading-Edge Separation From Slender Delta Wings.* Tech. Rep. No. 66070, British Royal Aircraft Establ., Mar. 1966.
8. Mendenhall, Michael R.; and Lesieutre, Daniel J.: *Prediction of Vortex Shedding From Circular and Noncircular Bodies in Subsonic Flow.* NASA CR-4037, 1987.
9. Mendenhall, Michael R.; and Perkins, Stanley C., Jr.: Vortex Cloud Model for Body Vortex Shedding and Tracking. *Tactical Missile Aerodynamics,* Michael J. Hemsch and Jack N. Nielsen, eds., American Inst. of Aeronautics and Astronautics, Inc., c.1986, pp. 519–571.
10. Bryson, A. E.: Symmetric Vortex Separation on Circular Cylinders and Cones. Trans. ASME, Ser. E: *J. Appl. Mech.,* vol. 26, no. 4, Dec. 1959, pp. 643–648.
11. Moore, Katharine: *Line-Vortex Models of Separated Flow Past a Circular Cone at Incidence.* Tech. Memo. Aero 1917, British Royal Aircraft Establ., Oct. 1981.
12. Rainbird, W. J.; Crabbe, R. S.; and Jurewicz, L. S.: *A Water Tunnel Investigation of the Flow Separation About Circular Cones at Incidence.* N.R.C. No. 7633 (Aeronaut. Rep. LR-385), National Research Council of Canada, Sept. 1963.
13. Milne-Thomson, L. M.: *Theoretical Hydrodynamics, Fifth ed. Revised.* Macmillan Press Ltd., 1968.
14. Wu, Jain-Ming; and Lock, Robert C.: *A Theory for Subsonic and Transonic Flow Over a Cone—With and Without Small Yaw Angle.* RD-74-2 (Proj. No. (DA) 1M262303A214), Tennessee Univ. Space Inst., Dec. 1973. (Available from DTIC as AD 776 374.)
15. Sarpkaya, Turgut: Separated Flow About Lifting Bodies and Impulsive Flow About Cylinders. *AIAA J.,* vol. 4, no. 3, Mar. 1966, pp. 414–420.
16. Batchelor, G. K.: *An Introduction to Fluid Dynamics.* Cambridge Univ. Press, 1970.
17. Föppl, Ludwig: *Vortex Motion Behind a Circular Cylinder.* NASA TM-77015, 1983.
18. Von Kármán, Th.; and Sears, W. R.: Airfoil Theory for Non-Uniform Motion. *J. Aeronuat. Sci.,* vol. 5, no. 10, Aug. 1938, pp. 379–390.
19. Sarpkaya, T.: An Analytical Study of Separated Flow About Circular Cylinders. Trans. ASME, Ser. D: *J. Basic Eng.,* vol. 90, no. 4, Dec. 1968, pp. 511–520.
20. Dyer, D. E.; Fiddes, S. P.; and Smith, J. H. B.: Asymmetric Vortex Formation From Cones at Incidence—A Simple Inviscid Model. *Aeronaut. Q.,* vol. XXXIII, pt. 4, Nov. 1982, pp. 293–312.
21. Chin, S.; and Lan, C. Edward: *Calculation of Symmetric and Asymmetric Vortex Separation on Cones and Tangent Ogives Based on Discrete Vortex Models.* NASA CR-4122, 1988.

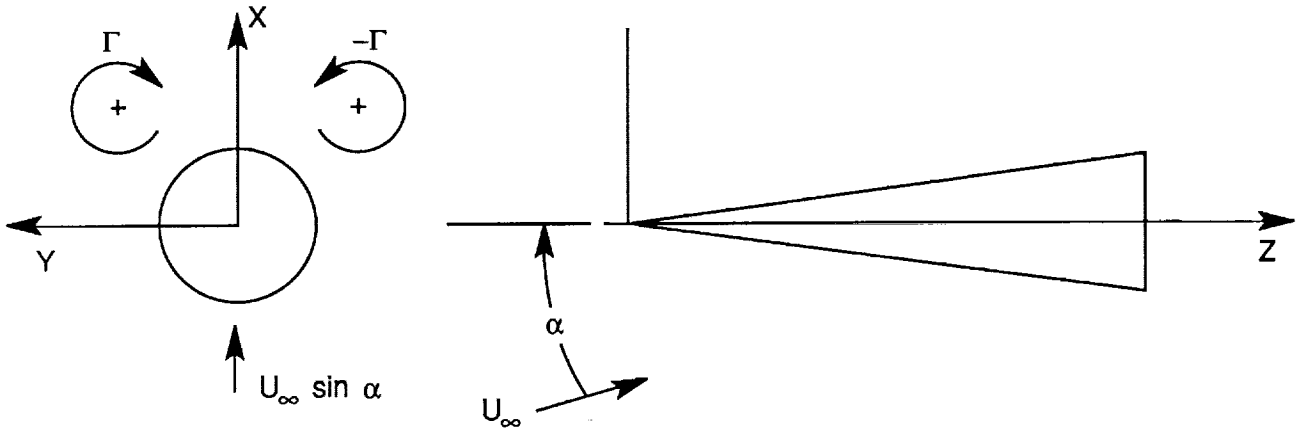

(a) System of axes.

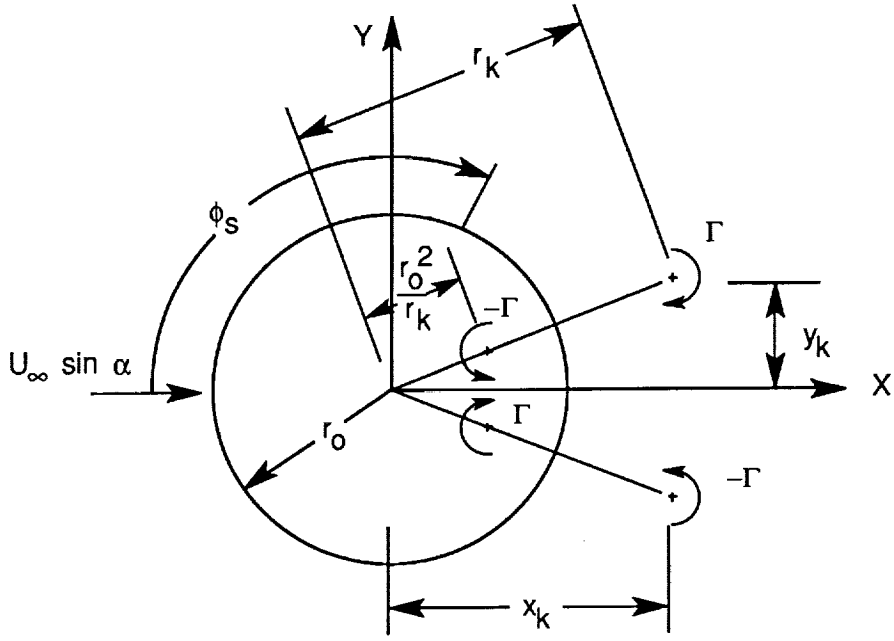

(b) Vortex-system geometry in crossflow plane.

Figure 1. Schematic of vortex-flow model.

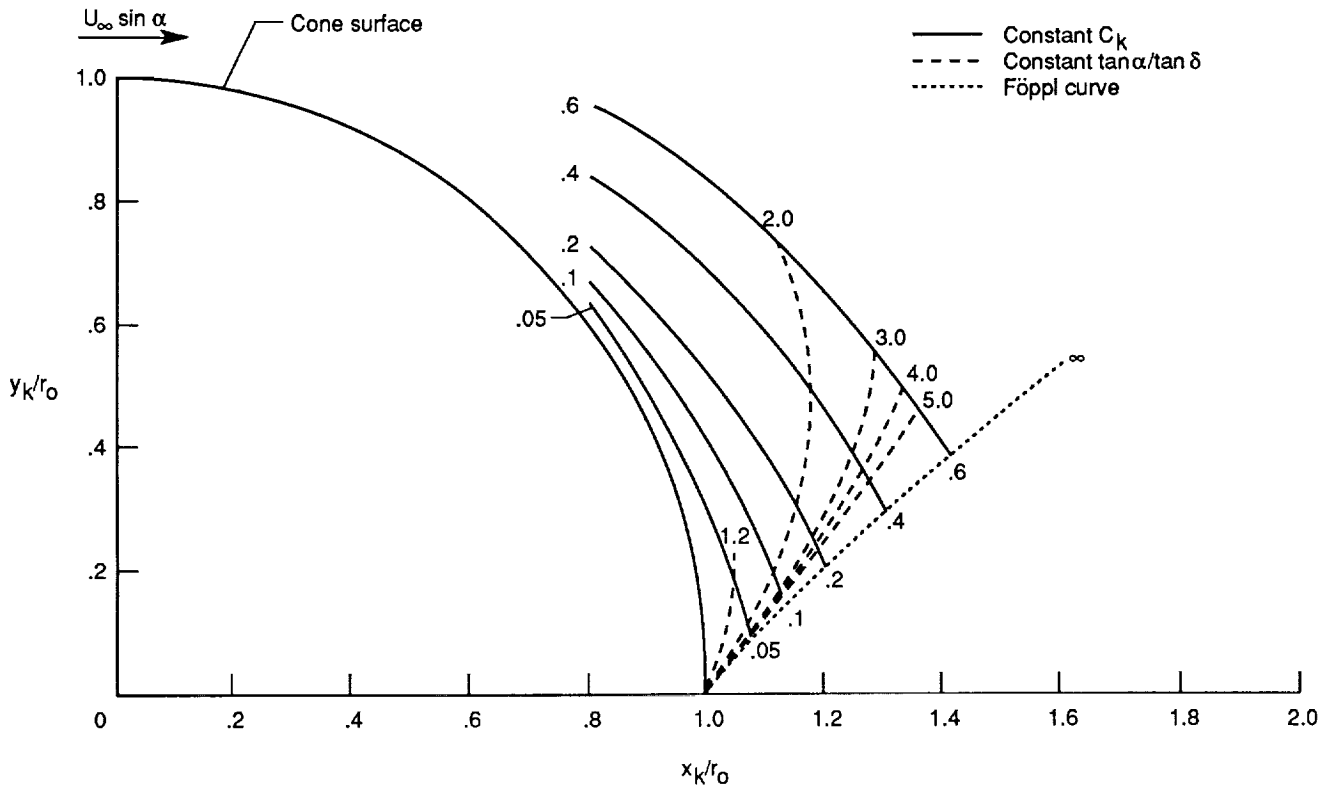

Figure 2. Solution field of vortex-center locations for different values of C_k and $\tan\alpha/\tan\delta$.

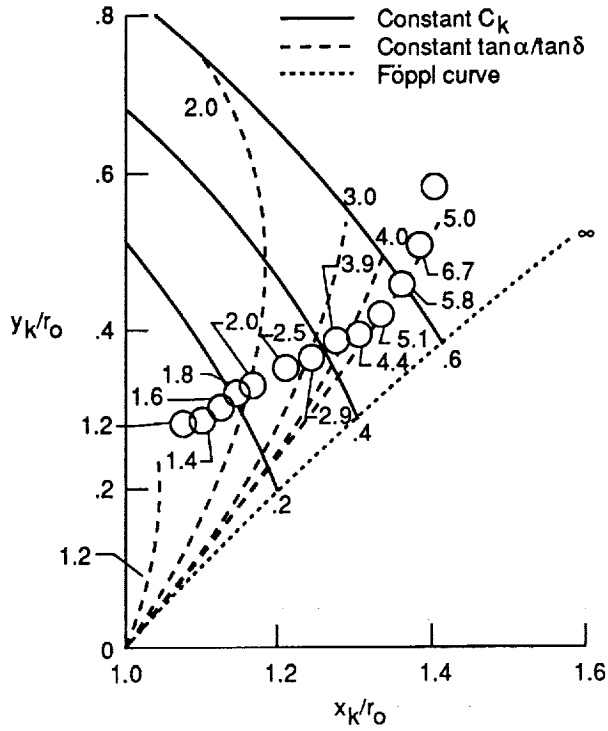

(a) $\delta = 7.5°$.

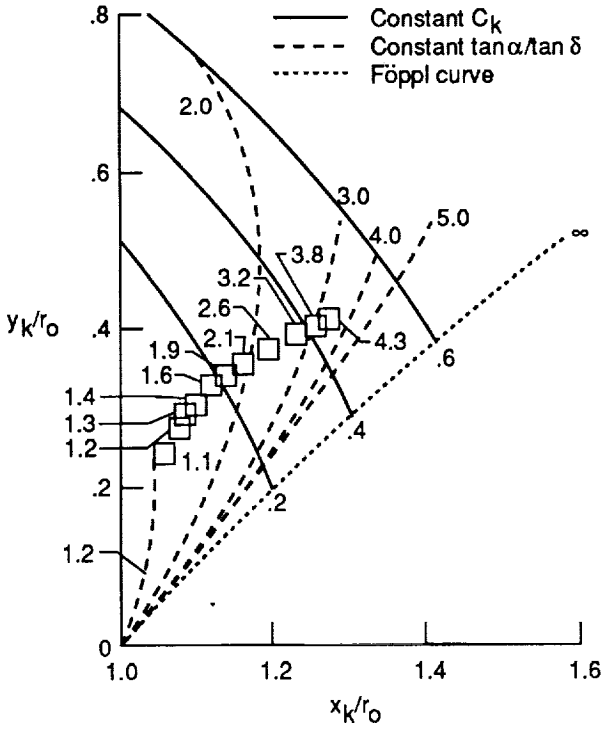

(b) $\delta = 12.5°$.

Figure 3. Comparison of calculated and measured vortex-center locations.

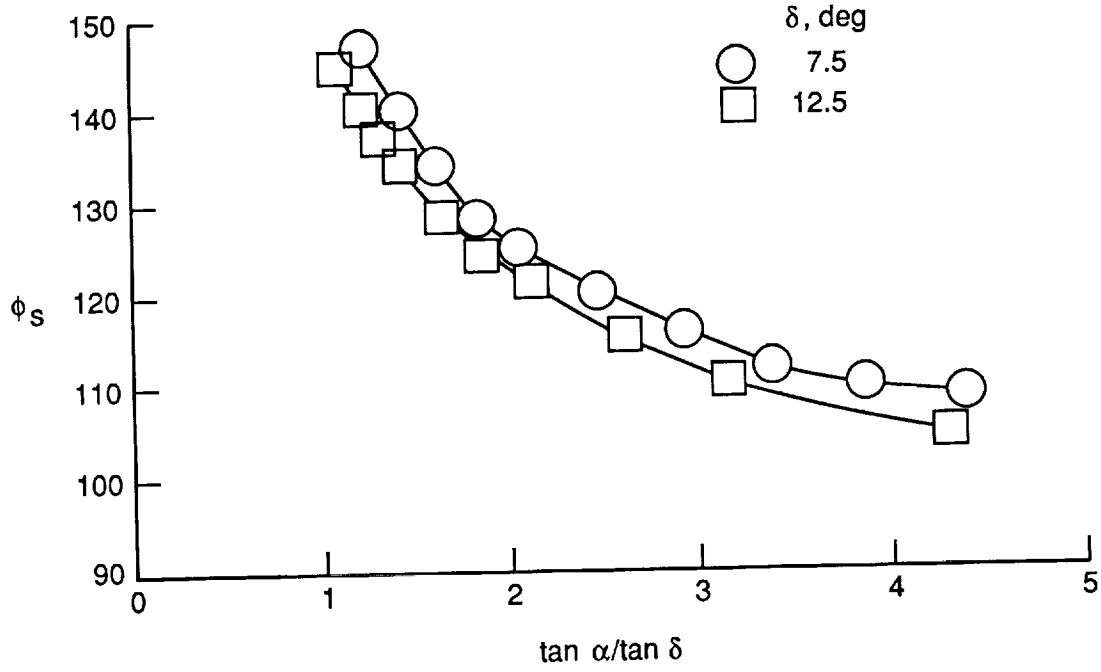

(a) ϕ_s versus $\tan\alpha/\tan\delta$.

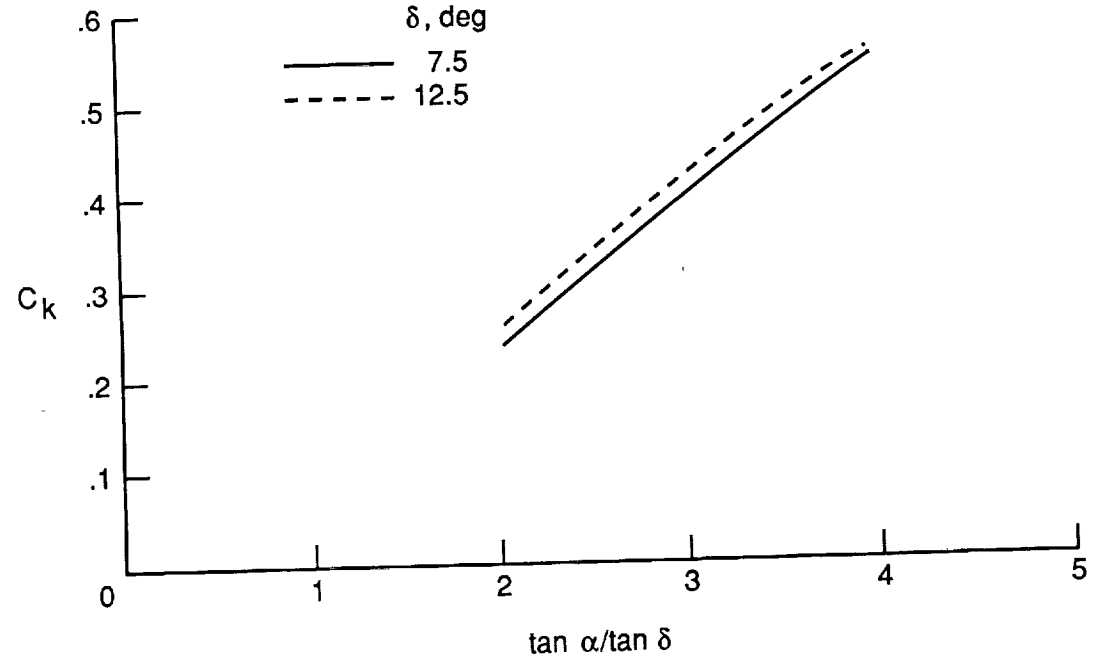

(b) C_k versus $\tan\alpha/\tan\delta$.

Figure 4. Variation of separation-point location and nondimensional vortex strengths with $\tan\alpha/\tan\delta$.

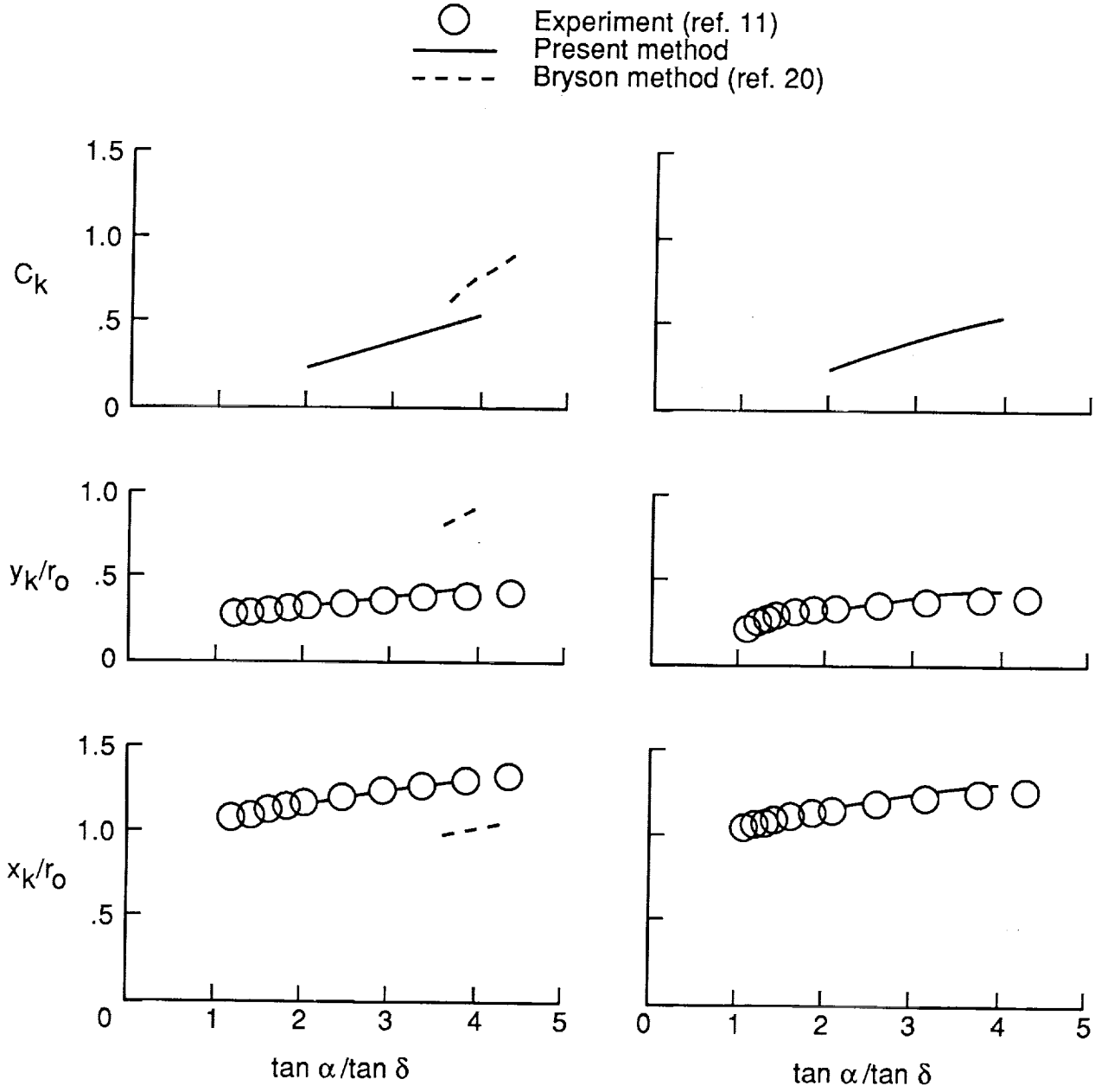

(a) $\delta = 7.5°$.

(b) $\delta = 12.5°$.

Figure 5. Nondimensional vortex strengths and vortex-center locations determined from experimental separation points given in figure 4(a).

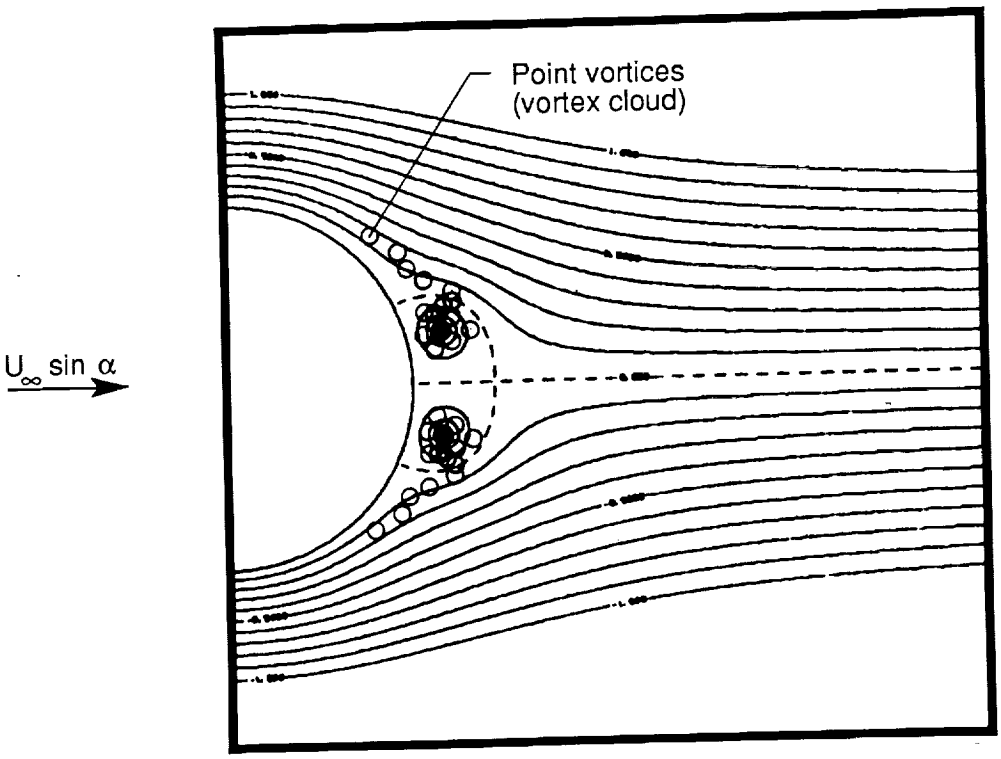

(a) $\alpha = 10°$.

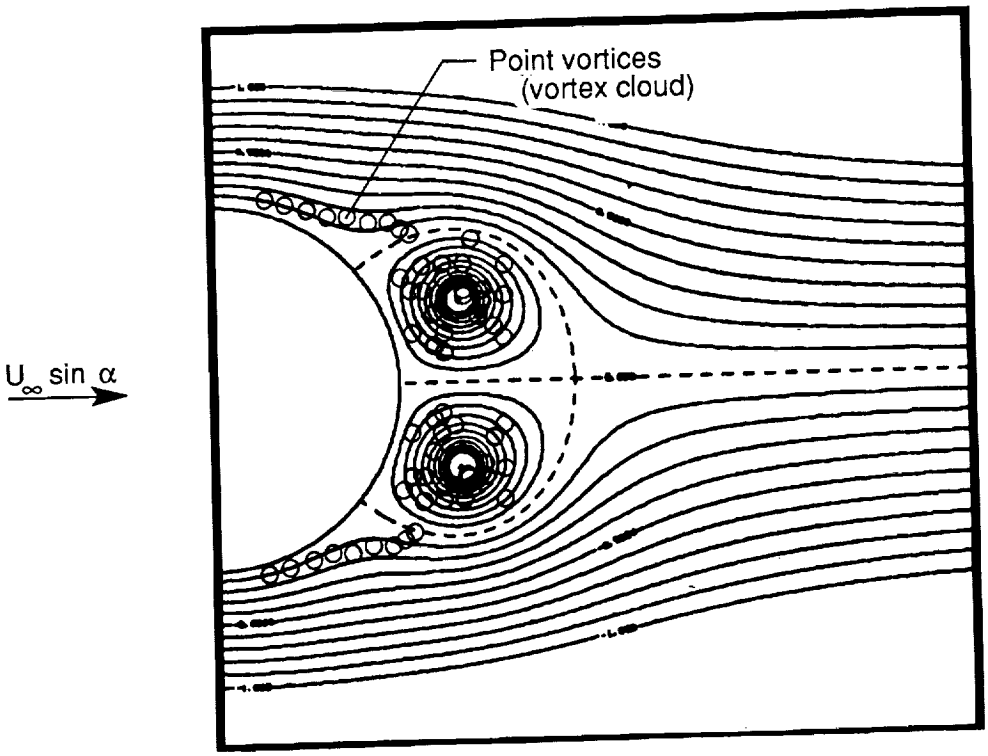

(b) $\alpha = 20°$.

Figure 6. Comparison of vortex rollup depicted by vortex cloud method (refs. 7 and 8) with streamlines calculated using present method. $\delta = 5°$.

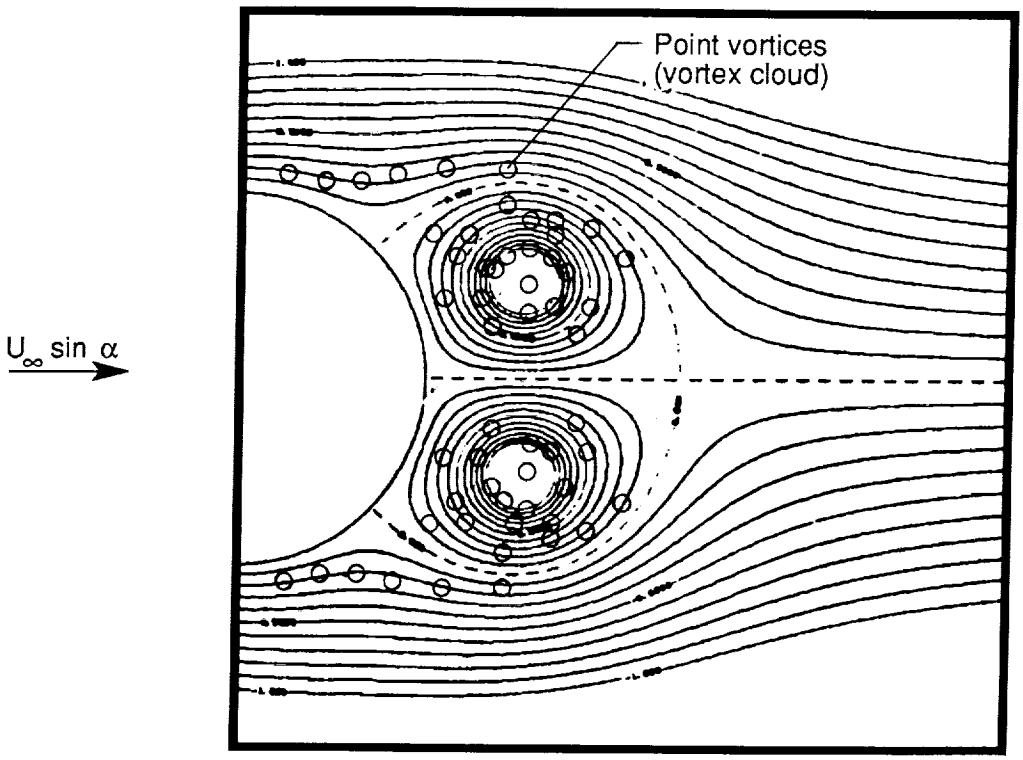

(c) $\alpha = 30°$.

Figure 6. Concluded.

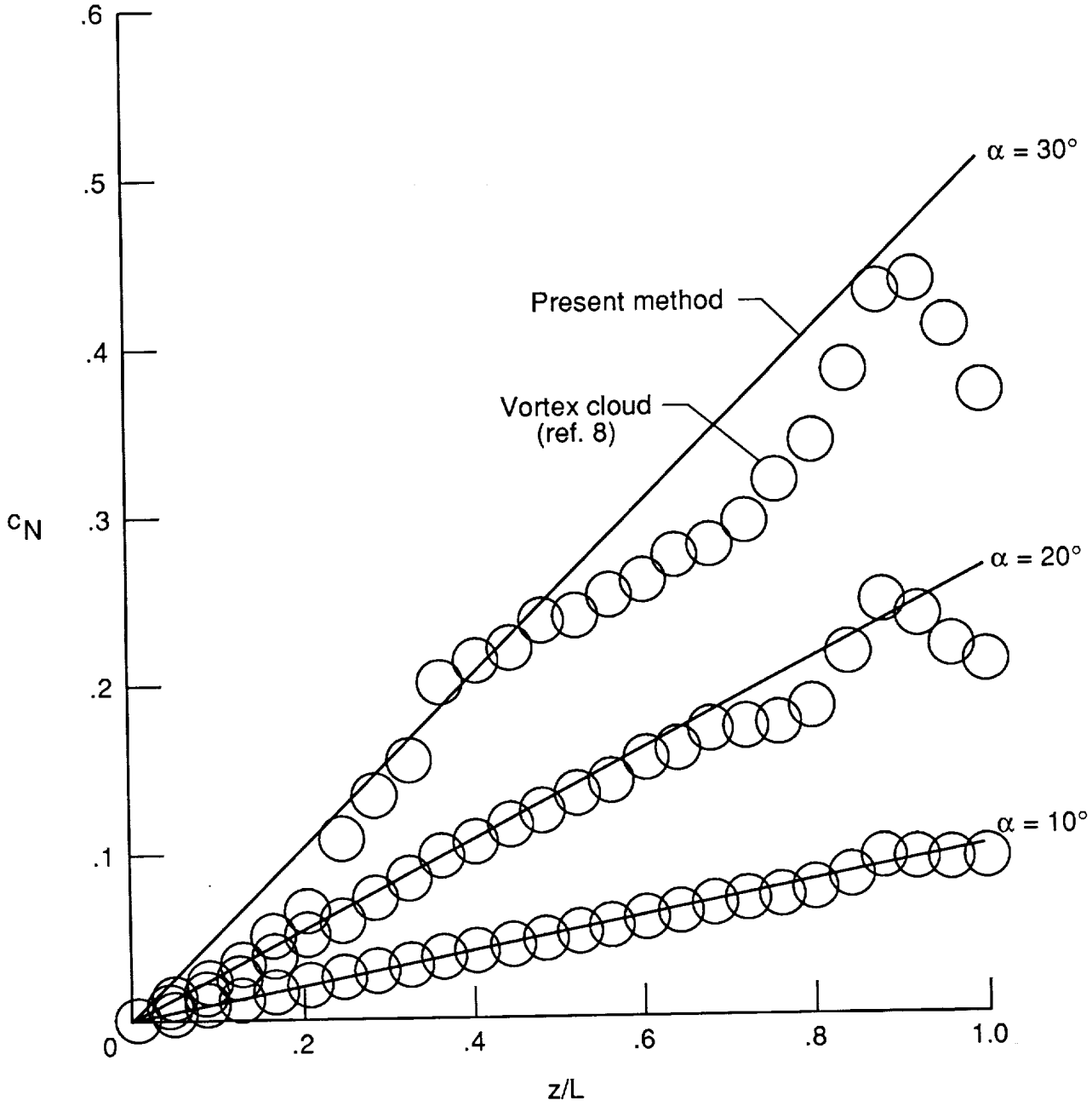

(a) $\delta = 5°$.

Figure 7. Comparison of local normal-force coefficients calculated using present method and vortex cloud method.

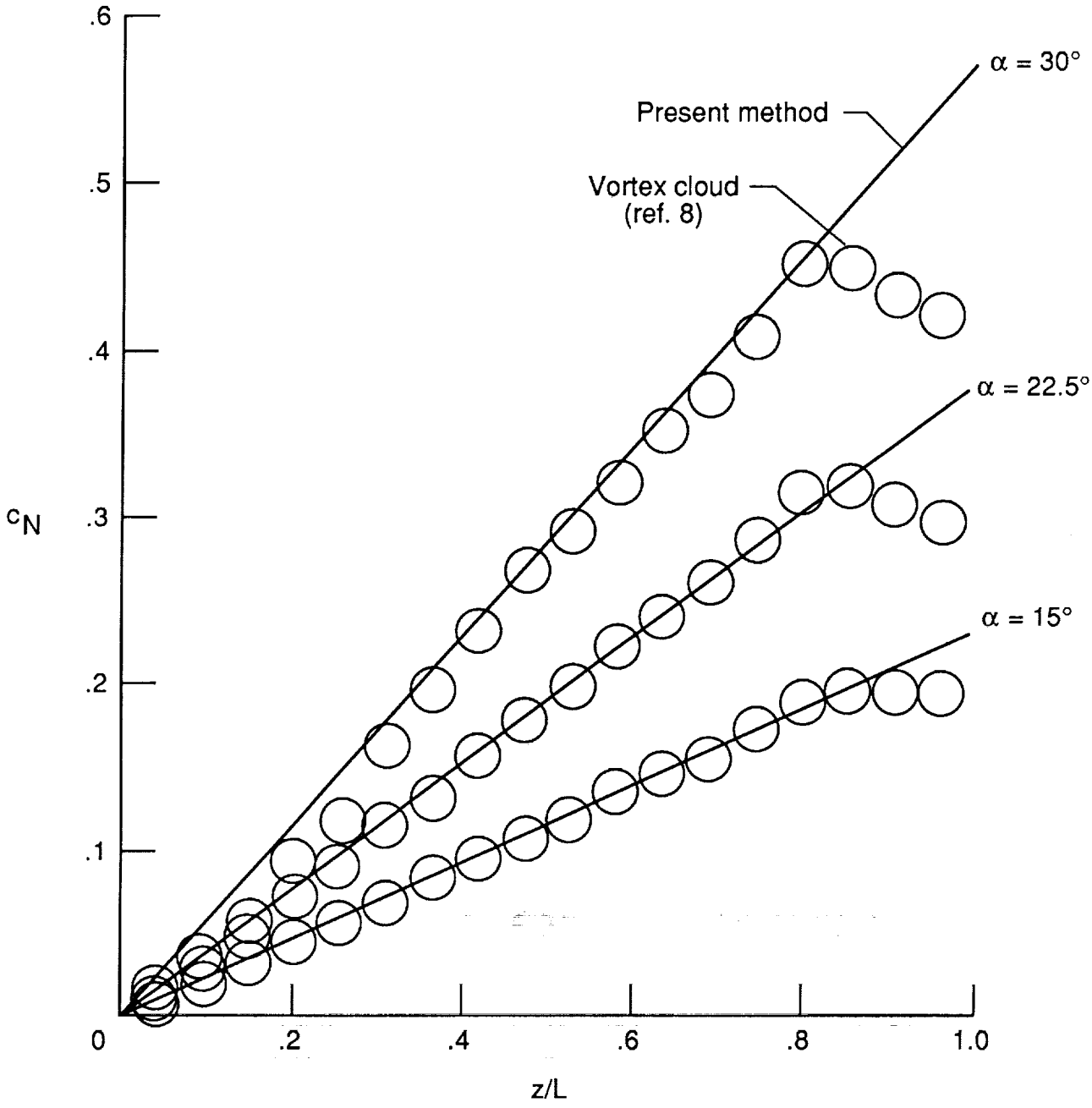

(b) $\delta = 7.5°$.

Figure 7. Concluded.

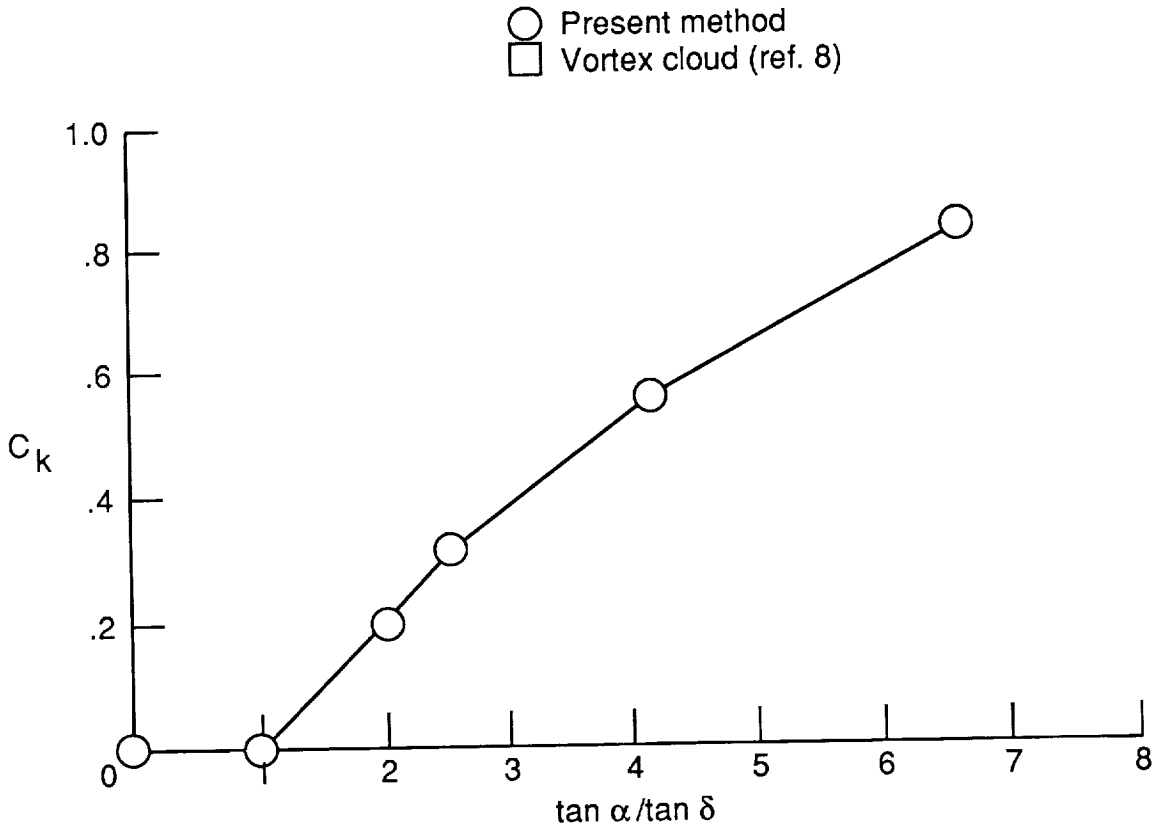

(a) C_k versus $\tan\alpha/\tan\delta$.

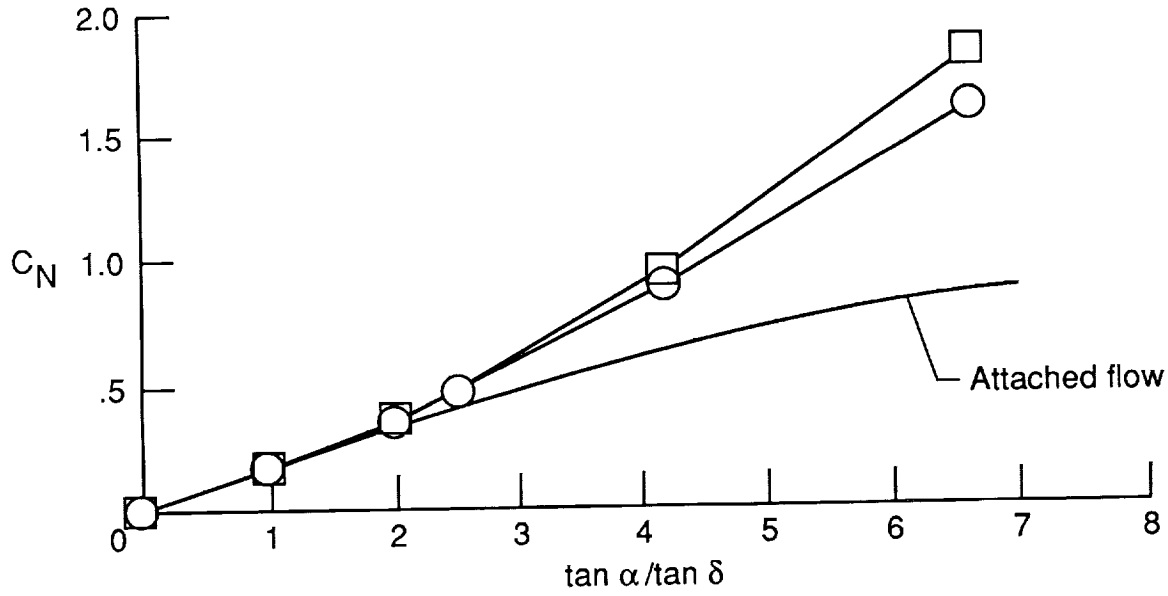

(b) C_N versus $\tan\alpha/\tan\delta$.

Figure 8. Comparison of total normal-force coefficients calculated using present method and vortex cloud method. $\delta = 5°$.

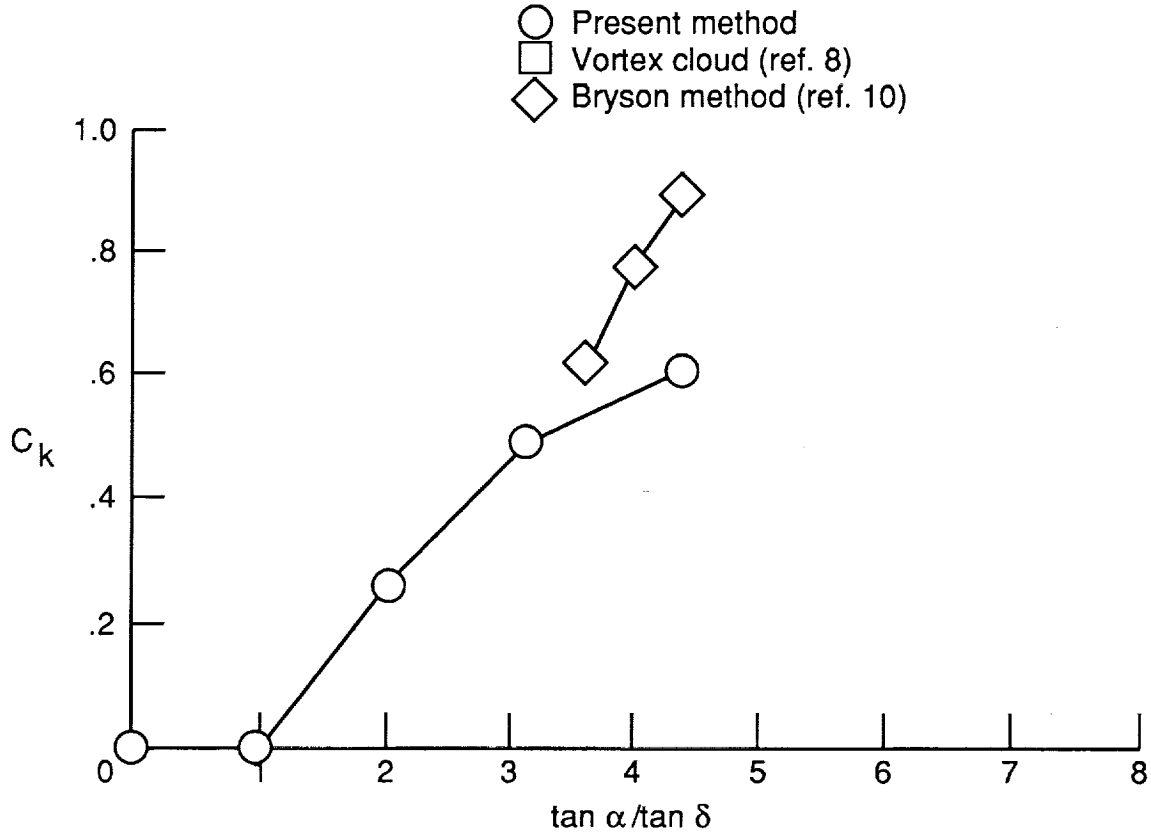

(a) C_k versus $\tan\alpha/\tan\delta$.

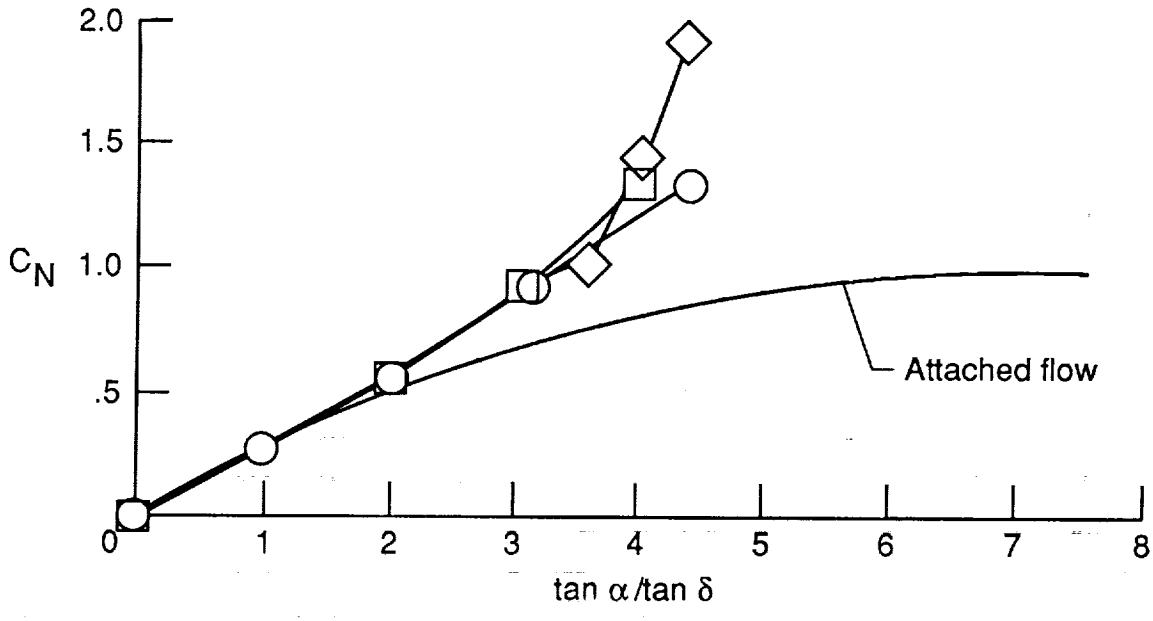

(b) C_N versus $\tan\alpha/\tan\delta$.

Figure 9. Comparison of total normal-force coefficients calculated using present method and vortex cloud method. $\delta = 7.5°$.

NASA
National Aeronautics and Space Administration

Report Documentation Page

1. Report No.	2. Government Accession No.	3. Recipient's Catalog No.
NASA TP-2989		

4. Title and Subtitle	5. Report Date
Discrete-Vortex Model for the Symmetric-Vortex Flow on Cones	May 1990
	6. Performing Organization Code
7. Author(s)	8. Performing Organization Report No.
Thomas G. Gainer	L-16586
	10. Work Unit No.
9. Performing Organization Name and Address	505-60-21-06
NASA Langley Research Center Hampton, VA 23665-5225	11. Contract or Grant No.
	13. Type of Report and Period Covered
12. Sponsoring Agency Name and Address	Technical Paper
National Aeronautics and Space Administration Washington, DC 20546-0001	14. Sponsoring Agency Code

15. Supplementary Notes

16. Abstract

A relatively simple but accurate potential-flow model has been developed for studying the symmetric-vortex flow on cones. The model is a modified version of the model first developed by Bryson, in which discrete vortices and straight-line feeding sheets were used to represent the flow field. It differs, however, in the zero-force condition used to position the vortices and determine their circulation strengths. The Bryson model imposed the condition that the net force on the feeding sheets and discrete vortices must be zero. The proposed model satisfies this zero-force condition by having the vortices move as free vortices, at a velocity equal to the local crossflow velocity at their centers. When the free-vortex assumption is made, a solution is obtained in the form of two nonlinear algebraic equations that relate the vortex-center coordinates and vortex strengths to the cone angle and angle of attack. The vortex-center locations calculated using the model are in good agreement with experimental values. The cone normal forces and center locations are in good agreement with the vortex cloud method of calculating symmetric flow fields.

17. Key Words (Suggested by Authors(s))	18. Distribution Statement
Aeronautics Aerodynamics	Unclassified—Unlimited Subject Category 02

19. Security Classif. (of this report)	20. Security Classif. (of this page)	21. No. of Pages	22. Price
Unclassified	Unclassified	27	A03

NASA FORM 1626 OCT 86

NASA-Langley, 1990

For sale by the National Technical Information Service, Springfield, Virginia 22161-2171